Temperature dependence of surface state lifetimes, dephasing rates and binding energies on Cu(111) studied with time-resolved photoemission

E. Knoesel, A. Hotzel and M. Wolf
Fritz-Haber-Institut der Max-Planck-Gesellschaft,
Faradayweg 4-6, D-14195 Berlin, Germany

(J. Electron. Spectrosc. Relat. Phenom., in press)

The ultrafast electron dynamics of surface states on Cu(111) is investigated as a function of temperature between 25 K and 460 K employing time-resolved two-photon photoemission (2PPE) spectroscopy. Analysis of the thermally induced energy shift of the unoccupied n = 1 image potential state based on a multiple reflection model allows a precise determination of the position of the upper edge (L_{6+}) of the *sp*-gap in the (111)-direction ($E_{L6+}(T) - E_F$ = 4.15 eV - (0.26 meV/K)T). We find that the lifetime of the n = 1 image state decreases from 22 ± 3 fs at 25 K to 14 ± 3 fs at 350 K. This is attributed to the increasing penetration depth of the image state wave function into the bulk at higher temperatures, where the image state crosses the band edge. The phonon contribution to the electronic dephasing of the n = 0 surface state and the n = 1 image state on Cu(111) is determined from their temperature dependent linewidths using three-level optical Bloch equations and is found to correlate with their wave function overlap with bulk states.

1. Introduction

The last few years have witnessed considerable progress in time-resolved studies of electronic excitations at surfaces with ultrafast laser techniques [1, 2]. In particular, time-resolved two-photon photoemission (2PPE) spectroscopy provides a powerful tool to probe the dynamics of photoexcited electrons with energy and momentum resolution on a femtosecond timescale. In 2PPE a first photon (pump pulse) excites an electron to a normally unoccupied state, from which it is subsequently photoemitted by a second photon (probe pulse). The photoelectron spectrum which is recorded as a function of the time delay between the pump and the probe pulse provides information about the lifetimes and relaxation dynamics in the intermediate state [3]. In the past, the majority of investigations employing time-resolved photoemission have focused on the dynamics of *energy relaxation* processes in bulk and surface states of semiconductors [2, 4-6] and metals [7-13]. However, for a complete understanding of the electron dynamics one has to elucidate also the *electronic dephasing*, which, for example, was found to play an important role in the excitation mechanism of surface states on Cu(111) [13, 14]. Recently, time-resolved

interferometric photoemission with optical phase resolution has been used for the first time to study the polarization and dephasing dynamics on a metal surface directly in the time domain [15]. It is the intention of this paper to analyze the influence of temperature on the energy and phase relaxation of surface states on Cu(111) and to separate the contribution of phonons from other dephasing processes. Previous studies have analyzed the photoemisson line shape of occupied states [16, 17], but the temperature dependence of the dynamics of *unoccupied* surface states on metals has not been investigated so far.

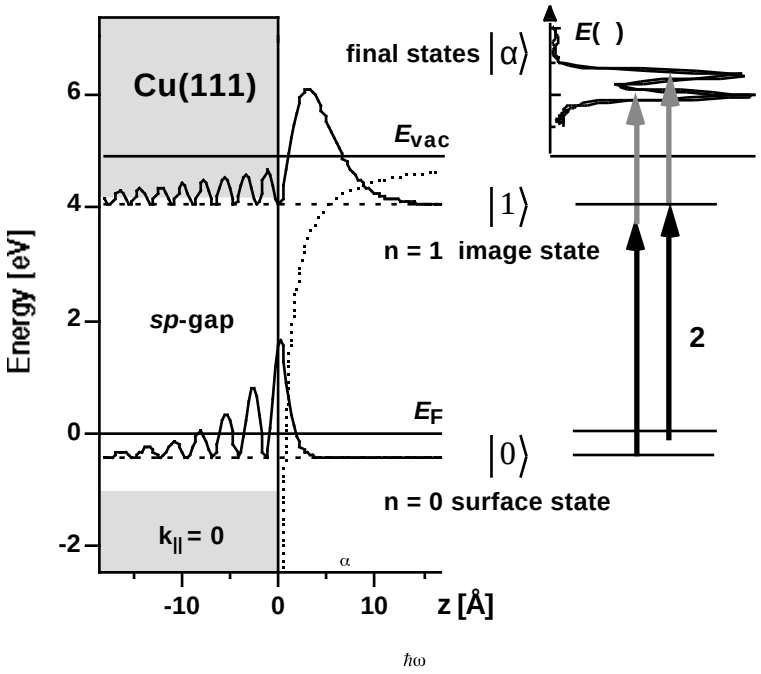

Figure 1: Electronic structure of Cu(111) for ($k_{\parallel} = 0$) and two-photon photoemission (2PPE). Left: The *sp*-gap of the projected bulk band structure (shaded) supports the occupied (n=0) surface state and the unoccupied (n=1) image potential state (solid curves display the probability density). Right: In 2PPE electrons are excited from the ground state |0> to the intermediate |1> and final states |α> by the pump ($2\hbar\omega$) and probe ($\hbar\omega$) laser pulses.

A particular class of surface states arises from the image potential in front of a metal surface if a gap in the projected bulk band structure prevents the escape of the electron into the crystal [18]. These image potential states form a Rydberg-like series of bound states below the vacuum level. Compared with energetically degenerate states in the bulk, image states have longer lifetimes because their wave function is localized mainly in front of the surface. Since the pioneering work of Steinmann [19] image states have been extensively studied with 2PPE spectroscopy (see Ref. [20] for a review). Here we focus on the Cu(111) surface, whose electronic structure is displayed schematically in figure 1 for zero parallel momentum ($k_{\parallel} = 0$). The *sp*-gap along the Γ-*L* line of copper supports the occupied n = 0 surface state, which lies 0.43 eV below the Fermi level (at 40 K) [21]. The first (n = 1) image state is located slightly below the upper edge of the *sp*-gap with a binding energy of 0.83 eV with respect to the vacuum level (at room temperature) [20]. The two sharp peaks in the 2PPE spectrum in figure 1 originate from a two-photon ($2\hbar\omega + \hbar\omega$) transition from the n = 0 state and a one-photon ($\hbar\omega$) excitation from the n = 1 state which is populated by the $2\hbar\omega$ pump pulse.

In figure 1 we show also the probability densities of the n = 0 and the n = 1 state. Note that the energetic position of the n = 1 state close to the band edge implies that its wave function penetrates deeply into the bulk where an excited electron is subject to various scattering processes (see fig. 1). As a consequence, the dynamical properties and binding energy of the image state depend critically on thermally induced energy shifts of the band edge. The temperature dependence of the *lower* edge of the *sp*-gap (labeled L_4-) is well known from photoemission studies ($E_{L4}(T) - E_F$ = -0.95eV + (0.33 meV/K)T) [22]. However, the *upper* band edge in the (111)-direction (labeled L_6^+) lies below the vacuum level ($\Phi_{Cu(111)}$ = 4.9 eV) and is thus not accessible as a final state in photoemission. Also previous inverse photoemission experiments [23] did not have sufficient energy resolution to determine $E_{L6^+}(T)$. The values for E_{L6^+} reported in the literature differ between 4.1 eV [24] and 4.25 eV above E_F [25].

In this paper we present a precise measurement of the temperature dependence of binding energies and linewidths of the n = 0 and n = 1 states on Cu(111) for zero parallel momentum ($k_{||}$ = 0). The analysis of the binding energies using the multiple reflection model reveals the thermally induced energy shifts of the *sp*-gap. We find that at low temperatures the n = 1 image state lies inside the gap but crosses the band edge above room temperature and becomes resonant with bulk states. This is accompanied by a substantial decrease of the image state lifetime as derived from time-resolved 2PPE experiments. The linewidth measurements combined with the time-resolved data allow to determine the so-called "pure" dephasing rates for the n = 0 and n = 1 states as a function of temperature. Our data indicate that the phase relaxation of surface states is determined by their probability density inside the crystal which also governs their coupling to phonons .

2. Experimental

The experiments were performed in an UHV chamber equipped with an electron time-of-flight spectrometer and a liquid helium cooled cryostat. A schematic overview of the experimental setup is shown in figure 2. For time-resolved 2PPE spectroscopy the output of a 200 kHz femtosecond Ti:Sapphire laser system (Coherent, Mira 900 and RegA 9000) pumping an optical parametric amplifier (Coherent, OPA 9400) is used. Tunable femtosecond pulses at a wavelength between 470 and 730 nm are obtained, which are compressed by a pair of SF10 prisms (GVD compensation) to a pulse duration between 50 fs and 80 fs depending on the wavelength used. From the visible OPA output second harmonic (2ω) pulses are generated in a 0.2 mm thick beta barium borate crystal and compressed by a pair of fused silica prisms. The 2ω and the visible pulse are delayed with respect to each other and overlapped nearly collinearly (skew <0.5°) on the sample with the electric field polarization parallel to the plane of incidence. The Cu(111) crystal is mechanically attached to the He-cryostat, and can be cooled down to 25 K. All 2PPE spectra were recorded along the surface normal ($k_{||}$ = 0) with 4.74 eV pump and 2.37 eV probe pulses.

The crosscorrelation between the pump and the probe pulses is measured in situ employing 2PPE from the n = 0 surface state [26] and reveals a pulse duration of 75±3 fs. A low pulse fluence (~10 μJ/cm^2) is used to exclude space charge broadening.

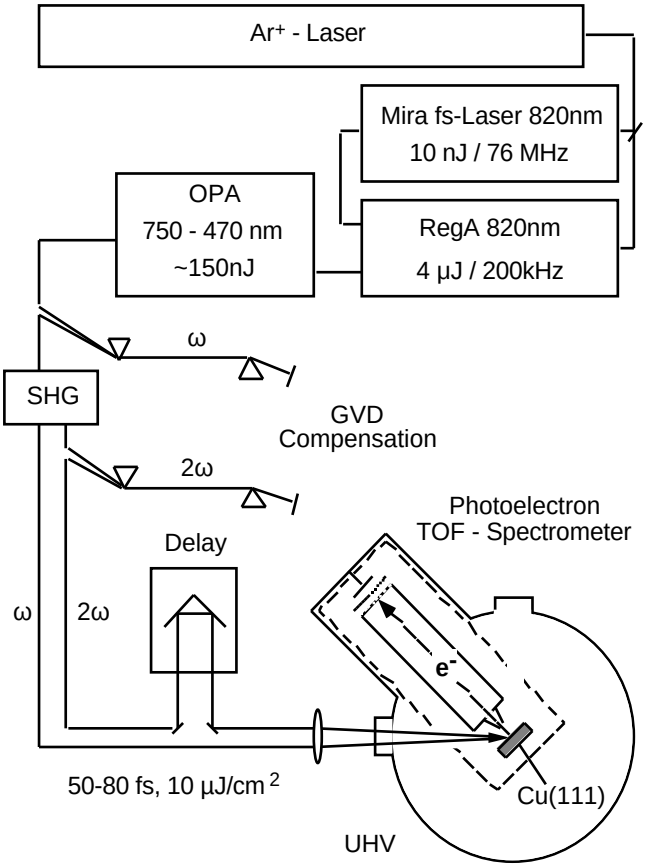

Figure 2: Experimental setup for time-resolved photoemission. An optical parametric amplifier (OPA) outputs tunable femtosecond laser pulses. which are delayed with respect to The second harmonic (SHG) pulses (2ω) are delayed with respect to the fundamental (ω) pulses and focused onto the Cu(111) sample. The photoelectrons are detected in a time-of-flight (TOF) spectrometer.

3. Theoretical analysis of time-resolved two-photon photoemission

Here we present a brief outline of the density matrix formalism, which is used to describe time-resolved two-photon photoemission spectroscopy of surface and image states on Cu(111) [14]. In our model we consider two discrete states, $|0\rangle$ and $|1\rangle$, which are coupled to an ionization continuum $|\alpha\rangle$ by the optical perturbation of the laser pulses. Initially the system is in the ground state $|0\rangle$, which represents the occupied n = 0 surface state on Cu(111) (see figure 1). The intermediate state, $|1\rangle$, corresponds to the normally unoccupied n = 1 image potential state and the final states $|\alpha\rangle$ are identified with the ionization continuum, where the electron leaves the surface with the kinetic energy $E(\alpha)$. These states are eigenstates of the Hamiltonian H_0 of the unperturbed system with $H_0|n\rangle = \hbar\omega_n|n\rangle$; $n = 0,1,\alpha$. The optical perturbation by the electromagnetic laser field is given by $V = er\ E_{pump}(t)\cos(\ _{pump}t) + er\ E_{probe}(t)\cos(\ _{probe}t)$ with the pulse envelopes $\vec{E}_p(t)$ and central frequencies ω_p of the pump and probe pulses, respectively. The external optical perturbation V creates a coherent superposition $|\Psi\rangle =$

$c_0(t)|0\rangle + c_1(t)|1\rangle + \sum_\alpha c_\alpha(t)|\alpha\rangle$ of the eigenstates of H_0, where the amplitudes and phase relations are given by the time-dependent coefficients $c_i(t)$. The time evolution can be calculated using density matrix theory, with the density operator $\rho = |\Psi\rangle\langle\Psi|$ [27, 28]. The population in each state $|n\rangle$ is then given by the diagonal element ρ_{nn} of the density matrix, while the off-diagonal elements represent the coherences between the levels. The response of this system to the optical perturbation V is obtained from the Liouville-von-Neumann equation:

$$\frac{d}{dt}\rho = -\frac{i}{\hbar}[H_0 + V, \rho] + \frac{d}{dt}\rho_{diss} \quad . \tag{1a}$$

Inserting the perturbation V and using the definitions $\tilde{\rho}_{kn} = e^{i(\omega_k - \omega_n)t}\rho_{kn}$ and $\left(\dot{\tilde{\rho}}_{diss}\right)_{kn} = e^{i(\omega_k - \omega_n)t}\left(\dot{\rho}_{diss}\right)_{kn}$ yields:

$$\begin{aligned} \dot{\tilde{\rho}}_{nn} &= -i\left(V_{nk}\tilde{\rho}_{kn} + V_{nm}\tilde{\rho}_{mn}\right) + cc. + \left(\dot{\tilde{\rho}}_{diss}\right)_{nn} \\ \dot{\tilde{\rho}}_{kn} &= iV_{kn}\left(\tilde{\rho}_{kk} - \tilde{\rho}_{nn}\right) - i\left(V_{km}\tilde{\rho}_{mn} - V_{mn}\tilde{\rho}_{km}\right) + \left(\dot{\tilde{\rho}}_{diss}\right)_{kn} \end{aligned} \qquad \text{with } k \neq n \neq m \neq k \tag{1b}$$

where $V_{nk} = \frac{1}{\hbar}\langle n|V|k\rangle e^{i(\omega_n - \omega_k)t}$. The dissipative term $\frac{d}{dt}\rho_{diss}$ in eq. 1 describes the energy and phase relaxation via the coupling to the continuum of substrate excitations on a phenomenological basis. These relaxation processes are mediated by (i) inelastic electron scattering leading to a decay of the population $\tilde{\rho}_{nn}$ with a rate Γ_n via electron-hole pair creation in the substrate and by (ii) (quasi)-elastic scattering (*e.g.* with phonons and defects), which leads to a decay of the coherence between the levels n and m with the so called 'pure' dephasing rate $\Gamma_{nm} = \Gamma_n + \Gamma_m$. The coupling between the final states $|\alpha\rangle$ can safely be neglected, because only transitions with frequencies ($\omega_n - \omega_k$) somewhere near the frequencies of the optical fields contribute to the 2PPE signal. Thus the problem reduces to solve a set of three-level systems where the final state energy $E(\alpha)$ is varied in order to calculate the theoretical photoelectron spectra from the final state populations $\tilde{\rho}_{\alpha\alpha}$. To keep the number of parameters small we neglect the energy relaxation in the final state (i.e. Γ_α=0) and thus obtain for the dissipative terms:

$$\frac{d}{dt}\left(\tilde{\rho}_{diss}\right)_{11} = -\Gamma_1\rho_{11} = -\frac{d}{dt}\left(\tilde{\rho}_{diss}\right)_{00} \tag{2a}$$

$$\frac{d}{dt}\left(\tilde{\rho}_{diss}\right)_{\alpha\alpha} = 0 \tag{2b}$$

$$\frac{d}{dt}\left(\tilde{\rho}_{diss}\right)_{01} = -\left(\Gamma_0 + \Gamma_1 + \frac{1}{2}\Gamma_1\right)\tilde{\rho}_{01} \tag{2c}$$

$$\frac{d}{dt}\left(\tilde{\rho}_{diss}\right)_{0\alpha} = -\left(\Gamma_0 + \Gamma_\alpha\right)\tilde{\rho}_{0\alpha} \tag{2d}$$

$$\frac{d}{dt}\left(\tilde{\rho}_{diss}\right)_{1\alpha} = -\left(\frac{\Gamma_1}{2} + \Gamma_\alpha + \frac{1}{2}\Gamma_1\right)\tilde{\rho}_{1\alpha} \qquad (2e)$$

The time evolution of the system is fully characterized by only four parameters, the energy relaxation rate Γ_1 of the n = 1 image state, and the 'pure' dephasing rates Γ_0^*, Γ_1^*, Γ_α^*. Note that similar to the evolution in the optical Bloch equations [28], the coherence is lost at half the rate at which population is transferred from $|1\rangle$ to $|0\rangle$ (see Eq. 2c and 2e). The above equations are thus also referred to as three-level optical Bloch equations [15]. In this scenario the intrinsic linewidth of the surface state is exclusively determined by the pure dephasing rate $\Gamma_0^* + \Gamma_\alpha^*$ between at which the coherence between the levels $|0\rangle$ and $|\alpha\rangle$ (i.e. the initial and final states) is lost. We note that the pure dephasing *rate* $\Gamma_0^* + \Gamma_\alpha^*$ corresponds to a intrinsic *linewidth* of $2\hbar$ $(\Gamma_0^* + \Gamma_\alpha^*)$ [27]. The linewidth of the n = 1 image state is given by $2\hbar$ $(\Gamma_1^* + \Gamma_\alpha^* + 1/2\,\Gamma_1)$, *i.e.*, both the image state lifetime $T_1 = 1/\Gamma_1$ and the 'pure' dephasing contribute. As has been demonstrated before for Xe/Cu(111) [3, 14], this formalism leads to a very good description of the 2PPE spectroscopy and dynamics of surface states on Cu(111).

4. Results and Discussion

Figure 3 displays 2PPE spectra for Cu(111) at various temperatures. The spectra are recorded with $2\hbar\omega$ = 4.74 eV pump and $\hbar\omega$ = 2.37 eV probe photon energies, where the 2PPE signal from the n = 0 state appears at higher kinetic energies (E_{kin}~1.8 eV) than the n = 1 state (E_{kin}~1.55 eV). The structure at E_{kin}~2.15 eV originates from the n =2 image state.

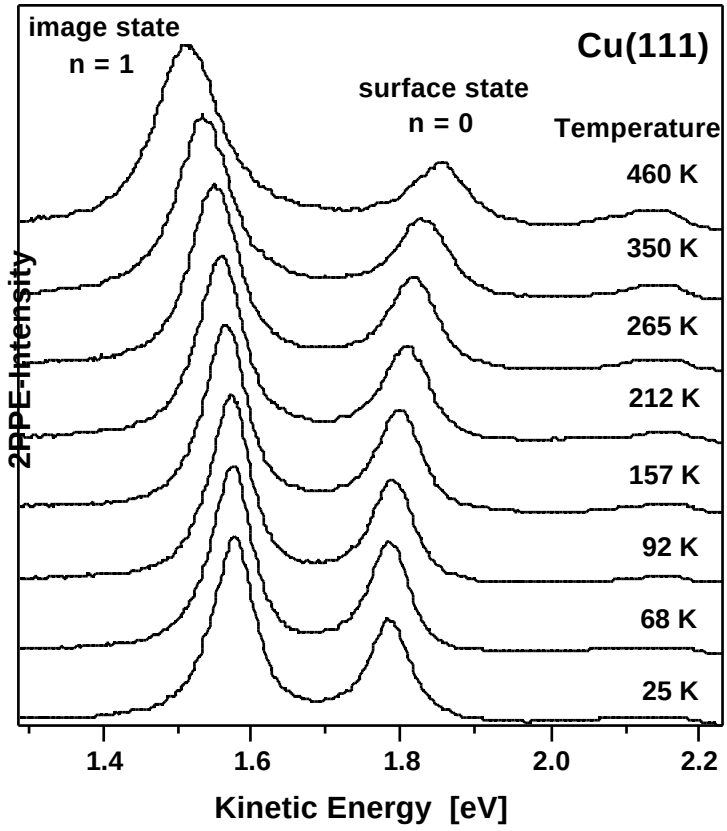

Figure 3: 2PPE spectra from Cu(111) for various temperatures taken with $2\hbar\omega$ = 4.74 eV pump and $\hbar\omega$ = 2.37 eV probe pulses. All spectra are normalized to the same maximum height [34]. The experimentally observed linewidths of the n=0 and n=1 state increase from 63 meV at 25 K to 100 meV at 460 K.

With increasing temperature the energetic positions of both the n = 0 and the n = 1 state shift and their linewidths increase. The experimentally observed linewidths (FWHM) are very similar for both states and increase from 63 meV at 25 K to 100 meV at 460 K. A similar albeit smaller increase in the width is also observed for the n =2 state. These measured linewidths include various contributions from the spectral width of the laser pulses (~17 meV), the spectrometer resolution (~8 meV) as well as the contribution from the energy and phase relaxation processes in the excited state. A more detailed analysis will be given further below.

Figure 4 shows the energetic position of the n = 0 and n = 1 state, which both shift towards the Fermi level with increasing temperature. For the n = 0 state we obtain a temperature coefficient of (0.18 ± 0.02) meV/K in agreement with previous studies [16, 21]. The binding energy of the n = 1 state (with respect to the vacuum level, $\Phi_{Cu(111)}$ = 4.9 eV) increases from 0.80±0.01 eV at 25 K to 0.85±0.01 eV at 400 K. The observed shifts can be attributed to the thermal expansion of the lattice, which leads to a narrowing of the *sp*-band gap. For a more quantitative analysis we use a one-dimensional multiple reflection model [18, 25] which has been

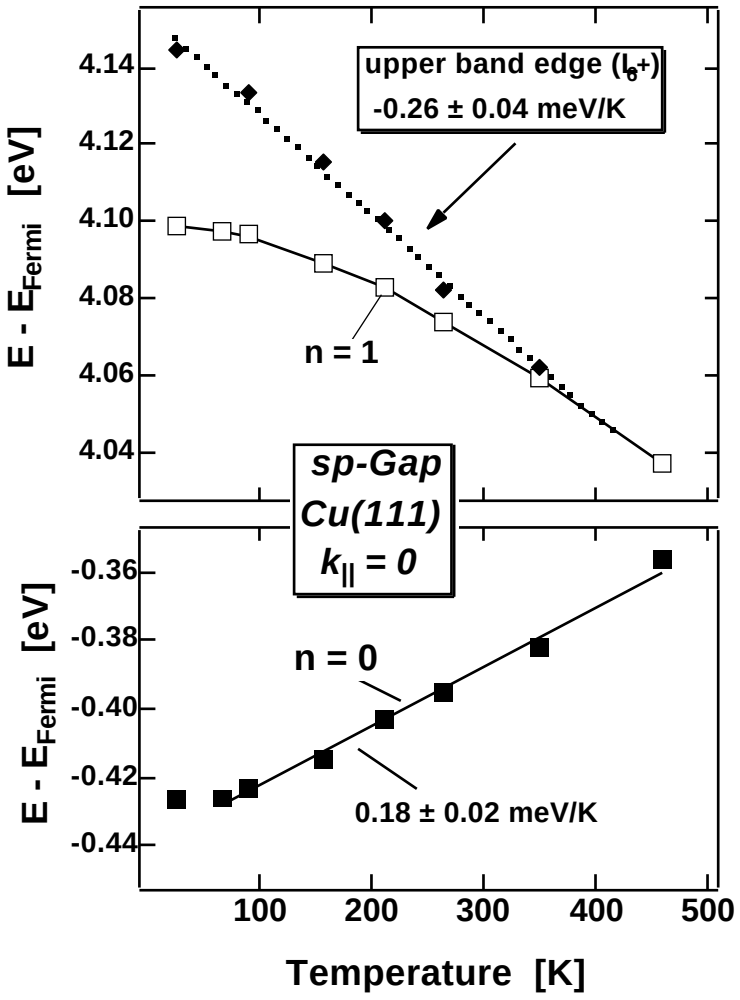

Figure 4: Upper panel: Energy of the n = 1 image state and the upper band edge (L_6^+) on Cu(111) with respect to E_F as a function of temperature. Lower panel: Binding energy of the n = 0 surface state versus temperature.

successfully used by Goldmann and coworkers to reproduce the temperature dependence of the occupied n = 0 states of the (111)-faces of noble metals [21]. The parameters which enter the calculation are $E - E_F$ = -8.6 eV are the bottom the *sp*-band [20] and the known temperature dependence of the lower band edge L_4- [22]. We then vary the position of the upper band edge to obtain optimum agreement with the measured binding energy of the n = 1 state. This reveals the temperature dependence of the upper band edge (L_{6+}) as $E_{L6+}(T) - E_F = 4.15\text{eV} - (0.26\ \text{meV/K})T$, which is of similar magnitude as the temperature coefficient of the lower band edge L_4- (+0.33 meV/K) [22].

The most striking result is that the n = 1 image state crosses the band edge around 400 K and comes in resonance with bulk states. This results in a substantial change of the penetration of the wave function into the crystal. We have calculated the n = 1 image state wave function by matching the solution of the nearly free electron model on the crystal side with the solution of Schrödinger's equation for the image potential on the vacuum side [20] and find that the part of the probability density of the image state inside the bulk increases from 25% at 25 K to about 60-70% at 350 K. In previous studies on Xe/Cu(111) we have shown that the image state lifetime is governed by the wave function penetration into the bulk and thus we expect a corresponding temperature induced change of the image state lifetime [13, 14]. The n = 1 lifetime was, therefore, investigated at different temperatures (namely 25 K and 350 K) using time-resolved 2PPE spectroscopy (not shown). For the analysis we follow a procedure where the cross-correlation signal at various final state energies is modeled together with the 2PPE spectrum using the three-level optical Bloch equations, as discussed elsewhere [3, 14]. We find that the lifetime of the n = 1 image state decreases from 22 ± 3 fs at 25 K to 14 ± 3 fs at 350 K. This correlates nicely with our previous measurement of 18 ± 5 fs obtained at 90 K [13]. Echenique and coworkers have calculated intrinsic linewidths (the inverse lifetime) of image states for (111)-faces of noble metals and found a nearly linear relationship between the linewidth $\Gamma = \hbar/\tau$ and the penetration of the wave function into the crystal [29]. According to de Andres *et al*. a penetration of 25% (as calculated for 25 K) would correspond to a lifetime $\hbar/\Gamma$ of 13 fs, whereas a penetration of 60-70% would yield 5-6 fs [29]. The observed trend of the n = 1 image state lifetime can thus be (at least semiquantitatively) explained by the increasing probability density inside the crystal with higher temperatures.

We now discuss the temperature dependence of the surface state linewidths and the role of phonons in the dephasing process. For the analysis of the spectra in figure 3 we use the three level Bloch equations to model the theoretical 2PPE spectra (as described in chapter 3). In the calculation we use the experimentally derived image state lifetime and the binding energies of the n = 0 and n = 1 state (from Fig. 4) as an input and adjust the 'pure' dephasing rates Γ_0^*, Γ_1^*, Γ_α^* to obtain optimum agreement with the experimental spectra. For those temperatures where

the image state lifetime was not determined by a direct measurement, we use a linear interpolation of the values given above [30]. From this analysis we derive the 'pure' dephasing rates Γ_0^*, Γ_1^* of the n = 0 and n = 1 state, which are plotted in figure 5 as a function of temperature. The dephasing rate Γ_α^* of the final states is found to be very small and we thus set $\Gamma_\alpha^* = 0$.

The pure dephasing rates (Fig. 5) combined with the image state lifetime allow to compare the intrinsic width of the n = 0 and n = 1 state with pervious work. For the n = 0 state we obtain at room temperature an intrinsic linewidth of 62±4 meV in agreement with previously reported values, which fall in the range between 55 meV [16, 31] and 65 meV [17, 32]. The intrinsic width of the n = 1 state is given by two contribution: (i) the pure dephasing (22 meV at room temperature) and (ii) the inverse lifetime, (about 40 meV at room temperature). The total intrinsic linewidth of 62±5 meV for the n = 1 image potential state is found to be smaller than the value of 85±10 meV reported by Fauster and coworkers [20, 32]. This may be attributed to the better energy resolution of our experiment or to a different surface quality, which might also affect the work function and hence the position of the image state with respect to the band edge.

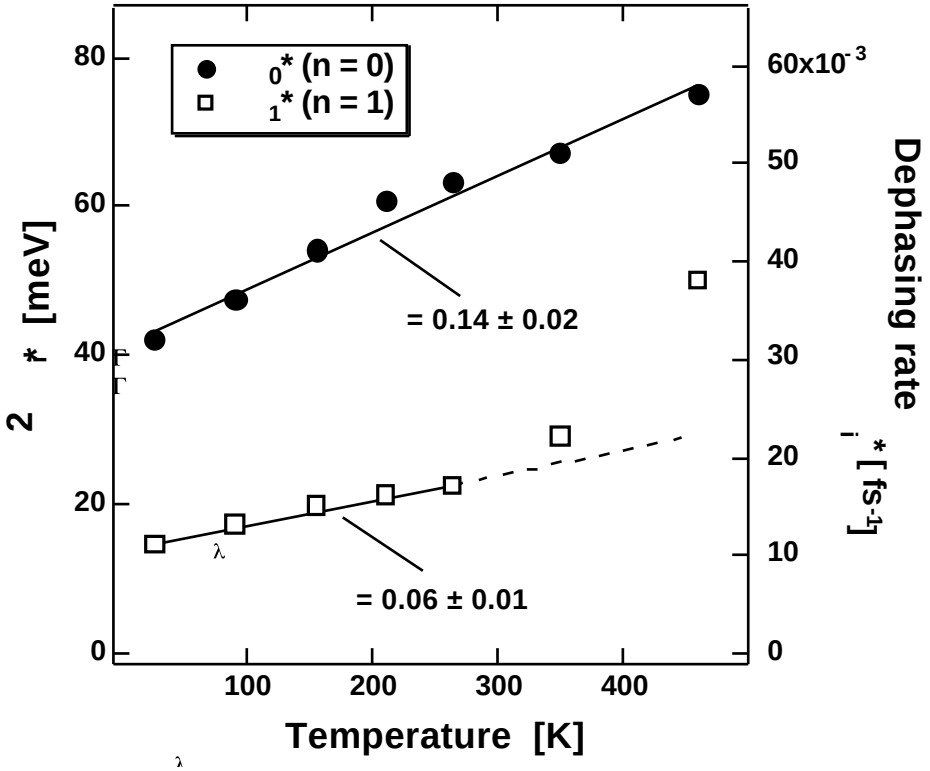

Figure 5: Right axis: Pure dephasing rates versus temperature derived from the linewidths of the n=0 and n=1 state using the optical Bloch equations. The left axis indicates the contribution from pure dephasing $2\hbar\Gamma_i^*$ to the intrinsic linewidth. The linear fits correspond to a mass enhancement parameter λ, derived from $W_{e\text{-}ph} = 2\pi\lambda k_B T$, of 0.14 and 0.06 for the n=0 and n=1 state, respectively. Note, that the dephasing rate of the image state increases strongly above 350 K where the n = 1 state crosses the band edge (see Fig. 4).

Figure 5 shows a linear increase of the intrinsic width of the n = 0 state with temperature, which extrapolates to 40 meV at 0 K. As demonstrated in Ref. [16] the phonon contribution to the intrinsic width can be described through the relationship $W_{e-p} = 2\pi\lambda k_B T$, where λ is the electron-phonon mass enhancement parameter, which connects the thermal electron mass m_{th} (determined from the electron specific heat) with the effective band mass m_b by $= m_b (1 + \lambda)$ [33]. Empirically the parameter λ can be regarded as a measure of the electron-phonon interaction strength. We find $\lambda = 0.14 \pm 0.02$ for the n = 0 state, which is in perfect agreement with the findings of McDougall *et al.* [16] and Matzdorf *et al.* [17]. The temperature independent fraction of the width (40 meV in our experiment) is attributed to scattering processes on small amounts of impurities or defects and to much lesser extend to the Auger decay of the photo-hole (<5meV) [16, 17].

For the n = 1 image potential state we observe also a linear temperature dependence for temperatures below 300K which would corresponds to a mass enhancement parameter $\lambda = 0.06 \pm 0.01$, *i.e.* only 40% of the value found for the n = 0 state. However, the increase of the dephasing rate Γ_1^* with temperature has to be interpreted with caution, because the penetration of the wave function into the crystal is also temperature dependent, which results in an increased probability for phase breaking scattering events with phonons and defects at higher temperatures. Indeed, we observe a pronounced increase of the dephasing rate Γ_1^* above 350 K where the image state crosses the band edge (see also figure 4). Interestingly we find that the pure dephasing rate Γ_1^* of the n = 1 state at zero temperature (14 meV by extrapolation to 0 K) amounts only 35 % of the rate Γ_0^* of the n = 0 state. This correlates nicely with the ratio between the probability densities of the two surface state inside the crystal. The occupied n = 0 state is located almost completely (85%) inside the crystal whereas the penetration of the n = 1 image state amounts only 25% at low temperatures (see figure 1). The photo-hole in the n = 0 state has, therefore, a higher probability to scatter with defects or phonons compared to an electron in the image state. Similar arguments were put forward by Matzdorf *et al.* [17] to explain value for the mass enhancement parameter $\lambda = 0.085 \pm 0.02$ for the Tamm state at $\overline{M}$ on Cu(111). This state is localized primarily in the topmost Cu layer and is thus less sensitive to the atomic vibrations compared to the n = 0 state at $\overline{\Gamma}$.

5. Conclusions

In summary we have investigated the temperature dependence of binding energies, lifetimes and linewidths of the n = 0 and n = 1 surface states on Cu(111) with time-resolved 2PPE spectroscopy. The binding energy of n = 1 image state was used to determine the position of the L_{6+} point in the band structure of copper ($E_{L6+}(T) - E_F = 4.15\text{eV} - (0.26\ \text{meV/K})T$) as a function of temperature. For the n = 1 image potential state we find a pronounced dependence of both the lifetime and the pure dephasing rate on the crystal temperature. This is explained by the

temperature dependent energy shifts of the bulk band structure, which results in an increasing penetration depth of the image state wave function into the bulk at higher temperatures.

Acknowledgment

Discussions with T. Hertel, P. Saalfrank and R. Matzdorf are gratefully acknowledged. We would like to thank G. Ertl for his generous and continuous support.

REFERENCES:

[1] P.F. Barbara, J.G. Fujimoto, W.H. Knox and W. Zinth (Eds.), Ultrafast Phenomena X, Springer, Berlin, 1996.

[2] R. Haight, Surf. Sci. Rep., 21 (1995) 275.

[3] M. Wolf, Surf. Sci., 377-379 (1997) 343.

[4] J.R. Goldman and J.A. Prybyla, Phys. Rev. Lett., 72 (1994) 1364.

[5] S. Jeong, H. Zacharias and J. Bokor, Phys. Rev. B, 54 (1996) R17300.

[6] N.J. Halas and J. Bokor, Phys.Rev. Lett., 62 (1989) 1679.

[7] W.S. Fann, R. Storz, H.W.K. Tom and J. Bokor, Phys. Rev. Lett., 68 (1992) 2834.

[8] C.A. Schmuttenmaer, M. Aeschlimann, H.E. Elsayed-Ali, R.J.D. Miller, D.A. Mantell, J. Cao and Y. Gao, Phys. Rev. B, 50 (1994) 8957.

[9] M. Aeschlimann, M. Bauer and S. Pawlik, Chem. Phys., 205 (1996) 127.

[10] E. Knoesel, A. Hotzel, T. Hertel, M. Wolf and G. Ertl, Surf. Sci., 368 (1996) 76.

[11] S. Ogawa, H. Nagano and H. Petek, Phys. Rev. B, 55 (1997) 10869.

[12] R.L. Lingle, N.H. Ge, R.E.Jordan, J.D. McNeill and C.B. Harris, Chem. Phys., 205 (1996) 191.

[13] M. Wolf, E. Knoesel and T. Hertel, Phys. Rev. B, 54 (1996) R5295.

[14] T. Hertel, E. Knoesel, A. Hotzel, M. Wolf and G. Ertl, J. Vac. Soc. Technol. A, 15 (1997) 1503.

[15] S. Ogawa, H. Nagano, H. Petek and A.P. Heberle, Phys. Rev. Lett., 78 (1997) 1339.

[16] B.A. McDougall, T. Balasubramanian and E. Jensen, Phys. Rev. B, 51 (1995) 13891.

[17] R. Matzdorf, G. Meister and A. Goldmann, Phys. Rev. B, 54 (1996) 14807.

[18] P.M. Echenique and J.B. Pendry, J. Phys. C, 11 (1978) 2065.

[19] W. Steinmann, Journal of Applied Physics A, 49 (1989) 365.

[20] T. Fauster and W. Steinmann. in: Electromangnetic Waves: Recent Development in Research, Eds. P. Halevi, (Elsevier, Amsterdam, 1995) p. 350.

[21] R. Paniago, R. Matzdorf, G. Meister and A. Goldmann, Surf. Sci., 336 (1995) 113.

[22] J.A. Knapp, F.J. Himpsel, A.R. Williams and D.E. Eastman, Phys. Rev. B., 19 (1979) 2844.

[23] W. Jacob, V. Dose, U. Kolac, T. Fauster and A. Goldmann, Z. Phs. B, 63 (1986) 459.

[24] R. Courths and S. Hüfner, Phys. Rep., 112 (1984) 53.

[25] N.V. Smith, Phys. Rev. B, 32 (1985) 3549.

[26] T. Hertel, E. Knoesel, M. Wolf and G. Ertl, Phys. Rev. Lett., 76 (1996) 535.

[27] R. Loudon, The Quantum Theory of Light, Clarendon Press, Oxford, 1983.

[28] C. Diels and W. Rudolph, Ultrashort laser pulse phenomena,
Academic Press, San Diego, 1995.

[29] P.L.d. Andres, P.M. Echenique and F. Flores, Phys. Rev. B, 35 (1987) 4529.

[30] Note that the evaluation presented in Ref. [14] was based on the assumption of a constant *(i.*e. temperature independent) image state lifetime.

[31] S.D. Kevan, Phys. Rev. Lett., 50 (1983) 526.

[32] W. Wallauer and T. Fauster, Surf. Sci., 374 (1997) 44.

[33] Grimvall, The electron photon interaction in metals, North Holland, Amsterdam, 1981.

[34] For a discussion of the dependence of photoemission intensities on temperature see:
R. Matzdorf, G. Meister and A. Goldmann, Surf. Sci., 286 (1992) 56.